

# The characteristics of the sensible heat and momentum transfer coefficients over the Gobi in Northwest China

Qiang Zhang,<sup>a\*</sup> Sheng Wang,<sup>a</sup> Michael Barlage,<sup>b</sup> Wenshou Tian<sup>c</sup> and Ronghui Huang<sup>d</sup>

<sup>a</sup> Gansu Province Key laboratory of Arid Climatic Changes and disaster Reduction, Institute of Arid Meteorology, China Meteorological Administration, Lanzhou 730020, People's Republic of China

<sup>b</sup> Institute of Atmospheric Physics, University of Arizona, Tucson, 85721, USA

<sup>c</sup> The School of Environment, University of Leeds, Leeds, UK

<sup>d</sup> Institute of Atmospheric Physics, Chinese Academy of Sciences, Beijing 100029, People's Republic of China

**ABSTRACT:** Utilizing the data of the intensive observation period (May–June 2000) of the Dunhuang land-surface process field experiment supported by the ‘Atmosphere-land Interactive Field Experiment over Arid Regions of Northwest China(NWC-ALIEX)’, the bulk momentum transfer coefficient ( $C_d$ ) and the bulk sensible heat transfer coefficient ( $C_h$ ) between the surface and the atmosphere over the arid Gobi Desert region are determined using three different methods. The results indicate that these coefficients, especially the means, are the same order of magnitude. The influence of the building near the observational station on the results is significant. When the building effect exists, the diurnal variation of the atmospheric bulk transfer coefficients and the bulk Richardson number are irregular. After the building effect is eliminated through analysing the wind direction, the bulk Richardson number and the range of the typical values of the bulk transfer coefficients over the Gobi are obtained. The diurnal variations of the bulk transfer coefficients are smoother than that without the building affect. The bulk transfer coefficients are larger in the daytime than in the nighttime. It is also worth noting that the variations of the bulk transfer coefficients and the bulk Richardson number are just opposite in phase, and that the bulk transfer coefficient for sensible heat flux is more related to the bulk Richardson number than that for momentum flux. The results are more reasonable than that after removing the building effect. The relation between the bulk transfer coefficients is also discussed. Copyright © 2010 Royal Meteorological Society

**KEY WORDS** Gobi; bulk transfer coefficient; bulk Richardson number; building effect

Received 9 June 2006; Revised 28 October 2008; Accepted 21 November 2009

## 1. Introduction

The momentum and heat transfer over land surfaces not only have notable implications for global climate change, but also are a key part of physical processes in atmospheric numerical models on various scales. At present, the land-surface fluxes in macro-scale models are obtained through the bulk transfer method, which requires the determination of bulk transfer coefficients (Stull, 1988). However, the bulk transfer coefficients used in most numerical models are not accurate. In arid regions, the bulk transfer coefficients on grid points in macro-scale models are not accurately provided due to a shortage of observations. The bulk transfer coefficients vary not only with different regions, but also with different times (Stull, 1988). Because of various reasons such as deriving methods and the observational problems, the estimated bulk transfer coefficients are often quite different even in the same region (Ye *et al.*, 1979; Li *et al.*, 2000; Zhao *et al.*, 2000).

The error in bulk transfer coefficients will cause proportional errors in surface fluxes and atmospheric models are then sensitive to these errors. Therefore, more accurate bulk transfer coefficients are necessary. The arid region of Northwest China, where an important surface feature is the Gobi (or desert), is very broad. The integrated contribution of its land-surface fluxes may have an effect not only on global climate change, but also on the East Asia monsoon circulation and the formation of the arid climate in Northwest China. Therefore, the observational study on the bulk transfer coefficients over the Gobi in Northwest China arid region is important both theoretically and practically.

From 1988 to 1992, a land-surface process field experiment in the arid region – Atmosphere-Land Surface Process Experiment at Heihe River Basin – was carried out in Gansu province in Northwest China by scientists from China and Japan(Gao, 1990). The results already obtained have improved our understanding and recognition on the land-surface process over the arid region (Wang *et al.*, 1991; Hu *et al.*, 1992, 1994; Zhang *et al.*, 1999). The primary attention of the experiment has been on the description of characteristics of land-surface processes

\*Correspondence to: Qiang Zhang, Institute of Arid Meteorology, China Meteorological Administration, No. 2070, Donggang East Road, Lanzhou, 730020, People's Republic of China.  
E-mail: Zhangqiang@cma.gov.ca

over desert and oasis surfaces. The analysis of the interaction between desert and oasis surfaces was another focus. The land-surface process studies over this region for macro-scale model parameterization schemes are relatively rare. Furthermore, the experimental area covered only the arid climate region where the annual precipitation is approximately 150 mm. It is not applicable to a more arid climate region where the annual precipitation is less than 50 mm.

In order to provide the surface flux parameterization scheme on the grid points in the Northwest China arid region, 'Land-Atmosphere Interaction Field Experiment in the Northwest China Arid Region' was carried out in Gansu and Qinghai provinces in May 2000. This experiment is one of the key field programs of a national project named 'Research on Formation Mechanism and Prediction Theory of Severe Climatic Disasters in China'. There is a permanent micrometeorological observation station at each of the three experiment sites, which are located in Dunhuang and Linzhe counties of Gansu province and Wudaoliang county of Qinghai province. An intensive observation experiment has already been carried out at the Dunhuang station from May 25th to June 17th (the Dunhuang Experiment). During this period, a micrometeorological station at Shuangdunzi Gobi near Dunhuang oasis, a PAM (Portable Automated Mesonet) station at Dunhuang Meteorological Station in oasis, and an automatic meteorological station at the transition area between the oasis and Gobi were established temporarily.

Meanwhile, the minisonde observations for more than 10 days in Dunhuang Meteorological Station, the supersonic fluctuation measurements, and a tethered balloon sounding was gathered for about 10 days in Shuangdunzi Gobi.

## 2. Observation field and data

The data analysed in this paper were observed during the Dunhuang Experiment at the Shuangdunzi Gobi micrometeorology station located at the west of the Dunhuang oasis (40°10'N, 94°31'E). The observational site is about 7 km from the edge of the oasis and 20–30 km from the south of Mount Mingsha with an elevation of 1150 m above sea level. The annual mean surface pressure of the station is 873 hPa and the annual precipitation is about 40 mm. The area is flat with a top soil layer being mainly pebble and the bottom being sand. The prevailing wind direction is easterly.

In the Dunhuang Experiment, the observations include winds, air temperature and humidity gradients on a tower, radiation components, surface and soil temperatures, air humidity in soil, soil heat fluxes and fluctuations of wind, temperature and humidity. The sensors of wind, temperature and humidity gradients on the tower were placed at four different heights (18, 8, 4 and 2 m). The wind direction instrument was installed at a 10-m height, and the radiation component instruments, including the direct radiation, the global radiation, the

Table I. The model and performance of the instruments.

Instrument	Country	Model	Factory	Performance
Wind direction sensor	China	FXI	Tianjin Meteorological Instrument Factory	Precision: 1.0°
Wind speed sensor	USA	10 228	BELFORT	Precision: 0.2 m/s(0.2~1.3 m/s), 0.22 m/s (1.3~22.0 m/s), 0.55 m/s (22.0~51.0 m/s)
Air temperature sensor	UK	Thermo-film 100 W30	Mathey Electronic	Sensitivity: 0.385 Ω/°C Response time: 3 s Precision: 0 °C, 0.05–0.08 Ω calibrated error: 0.1 °C
Air relative humidity sensor	Finland	HMP35A	VAISALA	Precision: ±2% RH (0–90% RH, +20 °C); ±3% RH (90–100% RH +20 °C)
Soil and surface temperature sensors	China	Pt100/A	Institute of Plateau Atmospheric Physics, C.A.S.	Precision: 0.1 °C
Soil water content sensor	USA	TDT		Precision: 1% Corrected precision: 0.1%
Soil heat flux plate	Japan	CN-81	EKO	Conductivity: $\lambda = 0.23 \text{ W}^{-1}/^{\circ}\text{C}$
Short-wave radiometer	Japan	MR-21	EKO	Precision: ±3%
Infrared radiometer	USA	PIR	Eppley	Precision: ±1%
Net radiation sensor	Japan	CN-11	EKO	Precision: ±3%
Supersonic fluctuation instrument	Japan	Kaijo-Denki	–	Error: 10%
Infrared hygrometer	Japan	DAT-300 Kaijo-Denki AH-300	–	Error: 20%

reflected radiation, the downward long-wave radiation and the upward long-wave radiation, were installed at a 1.5-m height. Three surface temperature sensors were spaced equally at 120° angles. The soil temperature was measured at six depths (5, 10, 20, 40, 80 and 180 cm) and the moisture sensors in the soil were measured at three levels (20, 40 and 80 cm). The soil heat flux plates were fixed at a 2.5- and 7.5-cm depth. The supersonic fluctuation sensors were at 2.9-m height and can give the means of momentum flux, sensible heat flux and latent heat flux every 30 min. Table I presents the specifications of the measurement instruments.

3. Computation method

The bulk transfer method for calculating surface fluxes can be written as (Zhao *et al.*, 1992)

$$\tau = 1/2\rho C_d V_a^2 \tag{1}$$

$$H = 1/2\xi - \rho c_p C_h (\theta_a - \theta_s) V_a \tag{2}$$

where  $\tau$  is the surface momentum flux,  $H$  is the surface sensible heat flux,  $\rho$  is the atmosphere density,  $c_p$  is the atmosphere specific heat,  $\theta_s$  is the surface potential temperature,  $V_a$  and  $\theta_a$  are atmosphere horizontal velocity  $((u^2 + v^2)^{1/2})$  and potential temperature (at 10-m height), and  $C_d$  and  $C_h$  are the momentum and sensible heat bulk transfer coefficients. The typical values of the bulk transfer coefficients range from about  $1 \times 10^{-3}$  to  $5 \times 10^{-3}$  (Stull, 1988). Those typical values only depend on the surface roughness length  $z_0$  under the condition of neutral stratified atmosphere. But usually they are also affected by a measure of atmospheric stability, such as the bulk Richardson number  $R_{ib}$  ( $R_{ib} = gz(\theta_a - \theta_s) \ln(z_a/z_0)/(TV_a^2)$ ). Therefore, the bulk transfer coefficients of wind and temperature can be expressed as

$$C_{d,h} = f_{d,h}(z_0, R_{ib}) \tag{3}$$

If the surface layer atmosphere obeys the Monin–Obukhov similarity theory and the Monin–Obukhov similarity functions are known, the above function can be written as (Zhao *et al.*, 1992)

$$C_d = [k/(\ln(z/z_0) - \psi_m)]^2 \tag{4}$$

$$C_h = k^2/[(\ln(z/z_0) - \psi_m)(\ln(z/z_0) - \psi_h)] \tag{5}$$

where  $\psi_m$  and  $\psi_h$  are the integration forms of the Monin–Obukhov similarity functions  $\phi_m$  and  $\phi_h$  to be given below,  $z$  is the height above ground,  $\kappa$  is the von Karman constant, and  $z_0$  is the roughness length. In reality,  $z_0$  is unknown, and  $\psi_m$  and  $\psi_h$  have some uncertainty. Rearranging Equations (1) and (2), the basic method for calculating the bulk transfer coefficients is

$$C_d = 1/2\tau/(\rho V_a^2) \tag{6}$$

$$C_h = 1/2\xi - H/(\rho c_p (\theta_a - \theta_s) V_a) \tag{7}$$

The bulk transfer coefficients can be obtained using different data and different methods to estimate the surface turbulent fluxes, which are calculated with three methods using the Dunhuang Experiment data.

3.1. Eddy correlation method

The eddy correlation method was used to directly calculate the surface turbulent fluxes with instantaneous fluctuations of wind and temperature observed by the supersonic instrument. It can be expressed as

$$\tau = \overline{u'w'^2} \odot + \overline{v'w'^2} \odot)^{1/2} \tag{8}$$

$$H = -\rho c_p (\overline{w'\theta'} + 0.84T\overline{w'q'}) \tag{9}$$

where  $T$  is the absolute temperature,  $u'$ ,  $v'$ ,  $w'$ ,  $\theta'$  and  $q'$  are meridional velocity, zonal velocity, vertical velocity, potential temperature and specific humidity fluctuation, respectively.

3.2. Aerodynamic method

The aerodynamic method calculates indirectly the turbulent flux with the gradients of wind speed, potential temperature and specific humidity between two levels (Zhang *et al.*, 1993). It can be expressed as

$$\frac{\kappa z}{u_*} \frac{\partial V}{\partial z} = \phi_m \tag{10}$$

$$\frac{\kappa z}{\theta_*} \frac{\partial \theta}{\partial z} = \phi_h \tag{11}$$

where  $u_*$  is the friction velocity ( $\tau \pm 1/2\rho u_*^2$ ),  $\theta_*$  is the turbulent temperature scale ( $H = -\rho c_p u_* \theta_*$ ),  $\kappa$  is the von Karman constant (0.4 usually), and  $z$  is the height.  $\phi_m$  and  $\phi_h$  are the Monin–Obukhov similarity functions of momentum and temperature. According to Dyer and Hicks (Dyer *et al.*, 1970; Hicks, 1976), their formulae are as follows:

$$\phi_m = \begin{cases} (1 - 16\xi)^{-1/4} & \xi \leq 0 \\ (1 + 5\xi) & \xi > 0 \end{cases} \tag{12}$$

$$\phi_h = \begin{cases} (1 - 16\xi)^{-1/2} & \xi \leq 0 \\ (1 + 5\xi) & \xi > 0 \end{cases} \tag{13}$$

where  $\xi$  is the Monin–Obukhov atmospheric stability (equals to  $z/L$ ,  $L$  is the Monin–Obukhov length), written as (Businger, 1988)

$$\xi = \begin{cases} 1.0R_i & R_i < 0 \\ R_i/(1 - 5R_i) & R_i \geq 0 \end{cases} \tag{14}$$

where  $R_i$  is the gradient Richardson number and given as:

$$R_i = \frac{g(z_1 z_2)^{1/2} (\theta_2 - \theta_1)}{T(V_2 - V_1)^2} \ln(z_2/z_1) \tag{15}$$

where  $g$  is the gravitational acceleration and the subscripts denote two different heights. From the above

equations, the roughness length can also be calculated by (Zhang *et al.*, 1996)

$$z_0 = z \times e^{-\frac{kV}{u_*} - \psi_m} \quad (16)$$

where  $V$  is the horizontal velocity at any level with height  $z$ . Theoretically, Equation (16) can be also used to compute the roughness length in the eddy correlation method and the combinatory method.

### 3.3. Combinatory method

The combinatory method (Thom *et al.*, 1975) is also an indirect method for calculating the surface turbulent fluxes with the gradients of wind, potential temperature and specific humidity as well as the surface radiation components and the soil heat flux. Hu *et al.* (1991) improved this method.

$$H = H_0 F \quad (17)$$

$$\tau = \tau_0 (F/\alpha) \quad (18)$$

where  $H_0$  and  $\tau_0$  can be expressed as

$$H_0 = -\rho c_p \kappa^2 z_i z_{i+1} \frac{\partial V}{\partial z} \frac{\partial \theta}{\partial z} \quad (19)$$

$$\tau_0 = \rho \kappa^2 z_i z_{i+1} \left(\frac{\partial V}{\partial z}\right)^2 \quad (20)$$

where  $F$  is a stratification influence function, and  $\alpha$  is the ratio of the momentum flux stratification influence function to the heat flux stratification influence function. The subscript  $i$  is the serial number of the levels at which the observational instruments were fixed.  $F$  and  $\alpha$  are expressed as

$$F = \frac{(R_n - G)}{H_0 + \lambda E_0} \quad (21)$$

$$\alpha = \begin{cases} F^{\frac{1}{3}} & \partial\theta/\partial z \leq 0 \\ 1.0 & \partial\theta/\partial z > 0 \end{cases} \quad (22)$$

where  $R_n$  is the surface net radiation,  $G$  is the soil heat flux and  $\lambda E_0$  given as:

$$\lambda E_0 = -\rho \lambda \kappa^2 z_i z_{i+1} \frac{\partial V}{\partial z} \frac{\partial q}{\partial z} \quad (23)$$

where  $\lambda$  is the latent heat of vapouration

In theory, the bulk transfer coefficients calculated from the eddy correlation method are the most accurate because the turbulent flux is measured directly. The aerodynamic method depends on the semi-empirical functions of Monin–Obukhov similarity and requires gradient data to be of good accuracy. In reality, the Monin–Obukhov similarity functions are somewhat different at different locations (Sorbjan, 1989) and the accuracy of gradient data is limited by observational technology. Though the combinatory method avoids using the Monin–Obukhov similarity functions, it requires gradient data of high quality and still has some theoretical limitation in calculating momentum flux.

## 4. Results

The data analysed in this paper are the hourly mean values of fluctuations, gradients, radiation components, surface temperature and soil heat flux. There are 445 h of data available including 10 days of 24-h data for analysing diurnal variation.

### 4.1. Mean of the bulk transfer coefficients

The first half Table II lists three sets of the averaged bulk transfer coefficients calculated by three different methods. The results show that the three sets are different implying that the values of the coefficients depend on the methods to some extent. However, their differences are small, especially the coefficients of the sensible heat.

If the bulk transfer coefficients calculated from the turbulent fluxes observed by the supersonic instrument were accurate, the difference between surface turbulent fluxes calculated by this method and others should be closely related to the measurement errors of the velocity, the potential temperature and the specific humidity. Accuracy for temperature is best, and that for humidity is the worst (Zhang *et al.*, 1992). Therefore, in the first half Table II, the difference in the sensible heat transfer coefficients calculated by different methods is the smallest

Table II. The averaged bulk transfer coefficients calculated by different methods after the building effect removed.

	Method	Momentum transfer coefficient, $C_d$	Sensible heat transfer coefficient, $C_h$	$C_d/C_h$	$C_{dn}/C_{hn}$
Before removing the building effect	<b>Eddy correlation method</b>	$2.50 \times 10^{-3} \pm 1.87 \times 10^{-3}$	$2.23 \times 10^{-3} \pm 1.12 \times 10^{-3}$	1.12	0.67
	Aerodynamic method	$1.16 \times 10^{-3} \pm 0.61 \times 10^{-3}$	$1.58 \times 10^{-3} \pm 1.04 \times 10^{-3}$	0.73	0.76
	Combinatory method	$1.78 \times 10^{-3} \pm 1.68 \times 10^{-3}$	$1.53 \times 10^{-3} \pm 1.08 \times 10^{-3}$	1.16	0.92
After removing the building effect	<b>Eddy correlation method</b>	$2.39 \times 10^{-3} \pm 1.57 \times 10^{-3}$	$2.10 \times 10^{-3} \pm 0.92 \times 10^{-3}$	1.13	0.50
	Aerodynamic method	$1.10 \times 10^{-3} \pm 0.48 \times 10^{-3}$	$1.45 \times 10^{-3} \pm 0.95 \times 10^{-3}$	0.76	0.67
	Combinatory method	$1.63 \times 10^{-3} \pm 1.68 \times 10^{-3}$	$1.49 \times 10^{-3} \pm 1.08 \times 10^{-3}$	1.10	0.85

4.2. Change of bulk transfer coefficient with bulk Richardson number

Figure 1 shows the variations of the atmospheric bulk transfer coefficients  $C_d$ (a) and  $C_h$ (b) calculated by the eddy correlation method with respect to the bulk Richardson number over Dunhuang Gobi. It shows that the tendencies agree with the theoretical results (Stull, 1988) and the orders of magnitude are also reasonable. From the second-order fitted curves of  $C_d$  and  $C_h$ , the neutral bulk transfer coefficients, which are the values when bulk Richardson number is equal to 0, are  $1.63 \times 10^{-3}$  and  $2.42 \times 10^{-3}$ . Those values are close to the results obtained from the desert and the Gobi in the Heihe region(Zuo *et al.*,1992).

The bulk transfer coefficients  $C_d$  and  $C_h$  calculated with the aerodynamic and combinatory methods over Dunhuang Gobi are similar to those calculated with the eddy correlation method, but the scatters are larger. This indicates that the eddy correlation method is the better method to calculate surface turbulent fluxes. So the discussion will focus on the characteristics of the bulk transfer coefficients calculated by the eddy correlation method.

4.3. The building effect on the experiment

Figure 2 shows the diurnal variation of the atmospheric bulk transfer coefficients  $C_d$ (a) and  $C_h$ (b) calculated by the eddy correlation method over Dunhuang Gobi. The variation of the bulk transfer coefficients is not significant

except in the morning hours from 4:00 to 9:00 (local time) and at dusk (only in  $C_h$ ). This suggests that some other factors not considered affect the bulk transfer coefficients.

In general, bulk transfer coefficients mainly depend on roughness length and the atmosphere stability. In order to understand the diurnal variation of bulk transfer coefficients, it is necessary to discuss the characteristics of roughness length and the atmosphere stability (such as the bulk Richardson number). Figure 3 shows the diurnal variations of the bulk Richardson number (a) and roughness length (b). It indicates that the diurnal variation of the bulk Richardson number is typical, but the roughness length is very special and abnormal. In general, the roughness length on the Gobi should be stable and constant. The periods marked by the abnormal roughness lengths appear to be in accordance with the abnormal bulk transfer coefficients. At night, because the feedback of atmosphere stability on the bulk transfer coefficients partly offsets the effect of the abnormal roughness length, the abnormal bulk transfer coefficients are not obvious. It was found that the abnormal roughness length was present mostly with a south wind.

Obviously, the abnormal roughness lengths were related to the buildings in the south of the observation station. Dunhuang Second Water Factory is about 130 m south from the tower. The factory had two 10-m-high storage tanks and some two-story buildings. They may

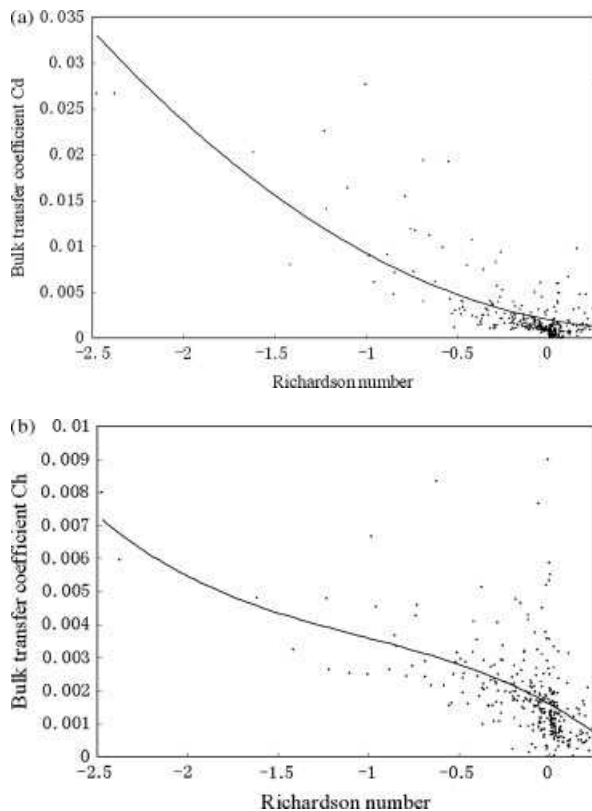


Figure 1. Change of the atmospheric bulk transfer coefficients  $C_d$ (a) and  $C_h$ (b) with the bulk Richardson number over Dunhuang Gobi.

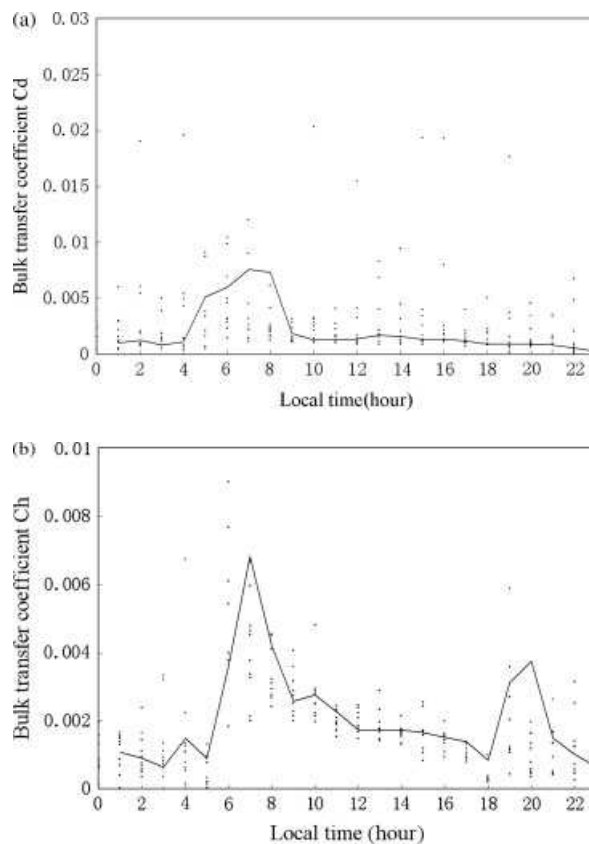


Figure 2. Diurnal variation of the atmospheric bulk transfer coefficients  $C_d$ (a) and  $C_h$ (b) estimated with the eddy correlation method over Dunhuang Gobi, the lines are fitted curves.

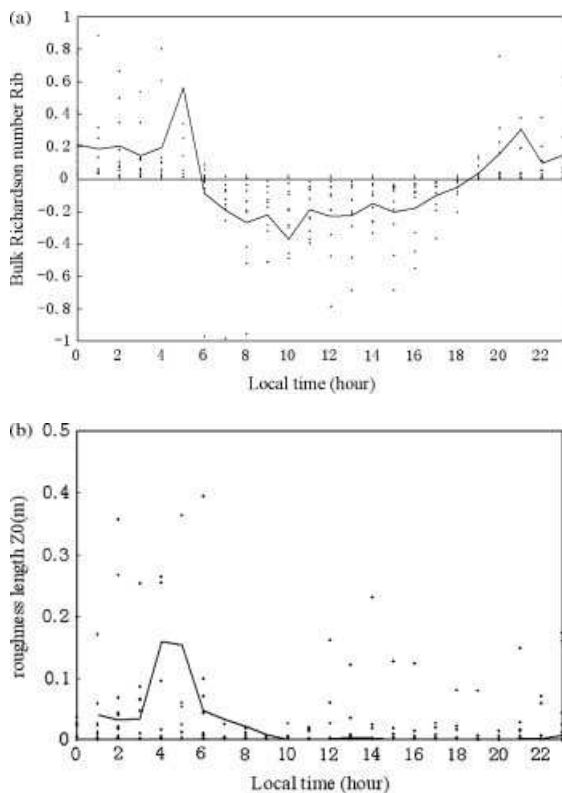


Figure 3. Diurnal variation of the bulk Richardson number (a) and roughness length (b), the lines are fitted curves.

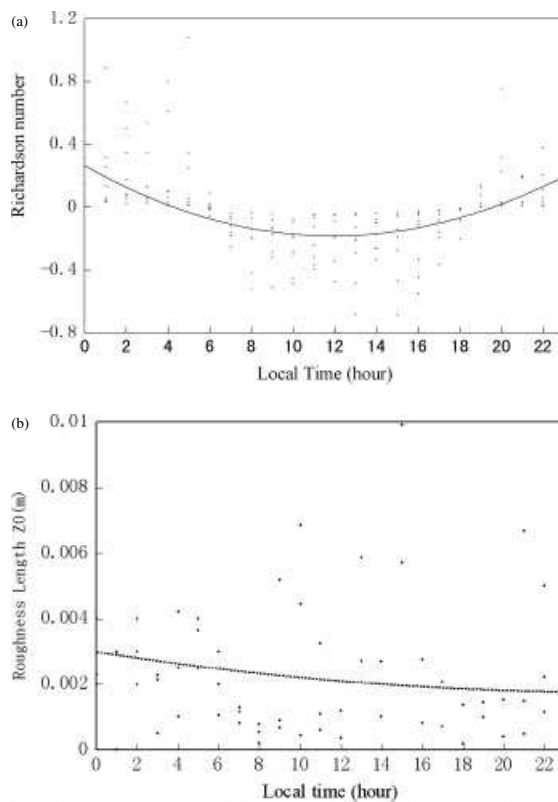


Figure 4. The same as the Fig. 3, but without the building effect, the lines are mean values.

be the main buildings that affect the results. In order to get general bulk transfer coefficients, the building effect must be eliminated. So the data with wind direction from 155° to 205° are removed in the following analysis

Figure 4 shows the diurnal variations of the bulk Richardson number and the roughness length after the building effect being removed. The diurnal variation of the bulk Richardson number becomes more typical and smooth, and the roughness length becomes more stable and constant. Although the effect on the roughness length is more evident, it is apparent that the buildings also have an effect on the bulk Richardson number.

#### 4.4. Bulk transfer coefficients after removing the building effect

Since the atmospheric bulk transfer coefficients are controlled by the bulk Richardson number and roughness length, the buildings may also indirectly affect characteristics of the atmospheric bulk transfer coefficients. Figure 5 displays the diurnal variation of the atmospheric bulk transfer coefficients  $C_d$ (a) and  $C_h$ (b) over Dunhuang Gobi with the building effect being removed. The diurnal variations of the bulk transfer coefficients also become more smooth. The bulk transfer coefficients are larger in the daytime than in the nighttime. It is also worth noting that the variations of the bulk transfer coefficients and the bulk Richardson number are just opposite in phase, and that the bulk transfer coefficient for sensible heat flux is more related to the bulk Richardson number than that for momentum flux. The results become more reasonable after the building effect are removed.

In the second half Table II presents three sets of averaged bulk transfer coefficients calculated with the three methods after the building effects are removed. Although the mean values do not significantly change compared with the values in the first half Table II, the values are smaller and more importantly so is the spread in the data.

Figure 6 shows the change of the atmosphere bulk transfer coefficients ( $C_d$  and  $C_h$ ) calculated by the eddy correlation method with the bulk Richardson number under unstable (a,b) and stable (c,d) atmospheric conditions after the building effects are removed. Note that the correlation between bulk transfer coefficients and  $R_{ib}$  is strong, especially under the unstable conditions. The tendency of their change with  $R_{ib}$  is near linear. Under unstable and stable atmosphere conditions, their secondary fitted formulae are:

$$C_d = \begin{cases} C_{dn}(1 + 12744.4C_{dn}R_{ib} - 32.6C_{dn}R_{ib}^2) & R_{ib} \leq 0 \\ C_{dn} & R_{ib} > 0 \end{cases} \quad (24)$$

$$C_h = \begin{cases} C_{hn}(1 + 616.6C_{hn}R_{ib} - 6.6C_{dn}R_{ib}^2) & R_{ib} \leq 0 \\ C_{hn}(1 - 2444.4C_{hn}R_{ib}) & R_{ib} > 0 \end{cases} \quad (25)$$

where  $C_{dn}$  and  $C_{hn}$  are the values of  $C_d$  and  $C_h$  under neutral condition, and are  $0.92 \times 10^{-3}$  and  $1.81 \times 10^{-3}$  respectively.

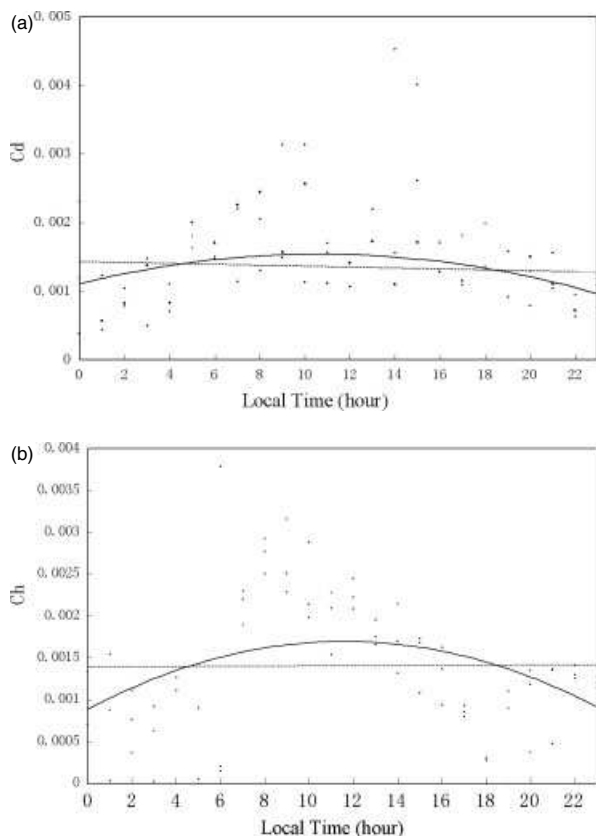


Figure 5. The same as Fig. 2, but without the building effect, the solid line is mean values.

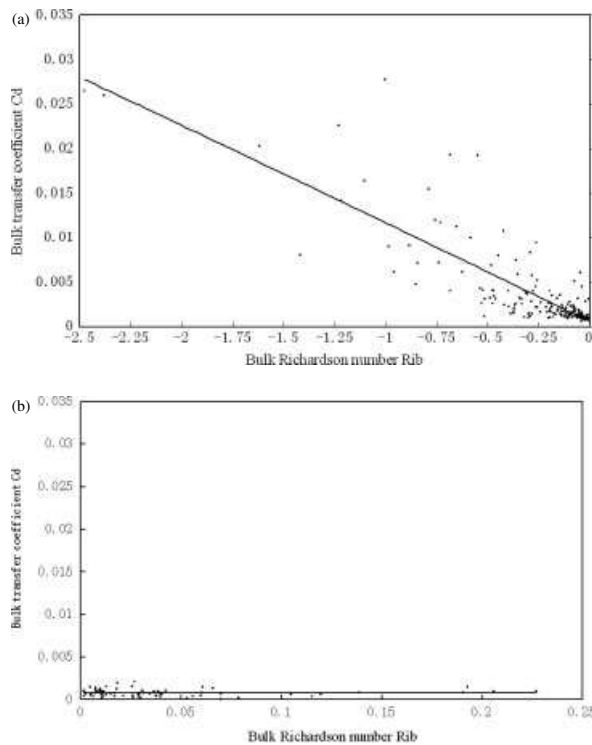


Figure 6. Change of the atmosphere bulk transfer coefficients ( $C_d$  and  $C_h$ ) with  $R_{ib}$  in unstable (a, b) and stable (c, d) states after the building effect being removed.

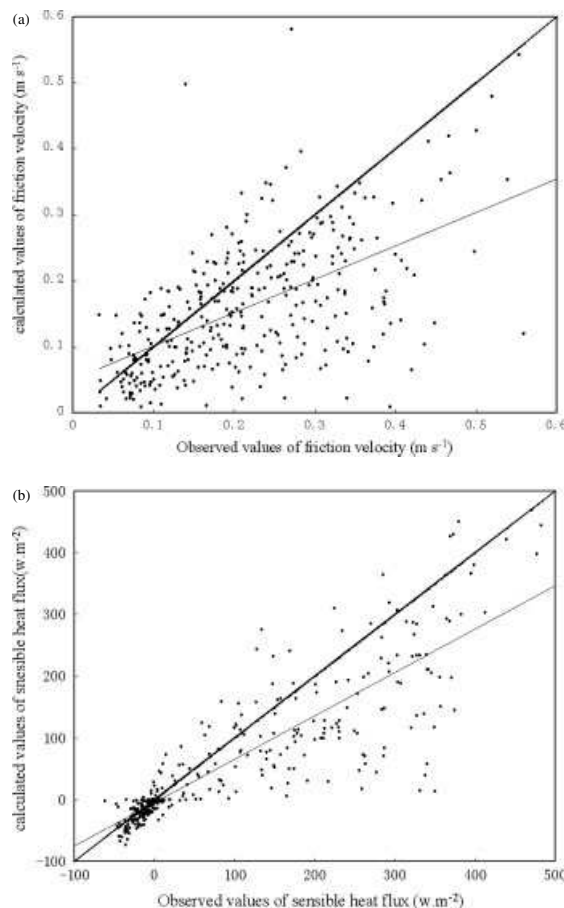


Figure 7. Comparison of friction velocity  $u_*$ (a) and sensible heat  $H$ (b) between the observed values and the values calculated with the fitted formulae.

4.5. Errors in the surface fluxes estimated by the bulk transfer coefficients

In order to test the effect of errors of the bulk transfer coefficient on the surface flux, the friction velocity  $u_*$  and the sensible heat flux  $H$  calculated by the fitted formulae (24) and (25) are compared with the observed values (Figure 7). It is shown that the averaged relative errors of the momentum and sensible heat fluxes are smaller than 20% and tolerable. When the friction velocity and the sensible heat flux calculated with the mean values of bulk transfer coefficients are compared with the observed ones, the relative errors of the fluxes calculated with the mean values are just about 2% larger than those with formulae (24) and (25). Table III lists the observed friction velocity and sensible heat flux along with and those calculated with the fitted formulae (24) and (25) and the averaged bulk transfer coefficients.

4.6. Characteristics of bulk transfer coefficients of arid regions

Because the climate and land-surface characteristics over the Gobi in arid regions are very different from those of the ocean, the plain, the plateau, etc. (Ha *et al.*, 1999; Yao, 1999), the bulk transfer coefficients must be of particular characteristics. The velocity affects indirectly the

Table III. A comparison between the observed friction velocity and sensible heat flux and those calculated with formulae (23), (24) and the averaged values.

	Friction velocity, $u_*$ $\text{ms}^{-1}$		Sensible heat flux, $H/W \text{ m}^{-2}$	
	Standard deviation	Residual variance	Standard deviation	Residual variance
Fitted formula	0.060	-0.038	37.4	-28.4
Average value	0.071	-0.025	42.6	-36.2

bulk transfer coefficients through the stratified stability over the Gobi, similar to those in the plain and plateau regions. But over the ocean, the surface roughness length are mainly controlled by wind speed, so the variation of the bulk transfer coefficients is directly affected by wind speed (Garratt, 1977). The latent heat transfer is small and the sensible heat transfer is dominant in arid regions, and hence, the sensible heat transfer coefficient is more important. The difference between the momentum roughness length and the scalar (temperature and humidity) roughness length over desert and the Gobi is very different from those over the ocean surface (Garratt, 1992) and moist land-surfaces. Differences also exist between the bulk transfer coefficients of the momentum and sensible heat fluxes. Due to the humid climate in the plain and the cold climate in the plateau, there is no obvious diurnal variation in the bulk transfer coefficients. But in arid regions, the solar radiation is intense and the soil thermal capacity is small, so that its surface is heated much more quickly than a moist land-surface. Thus, the diurnal variation (of what) under stably stratified conditions is more obvious, and the same is true for the bulk transfer coefficients. The obvious diurnal variation is one of the key characteristics of the bulk transfer coefficients over desert and the Gobi. Figure 8 shows the comparison of the diurnal variations of the momentum bulk transfer coefficients over the Gobi in the arid region and those over the Qinghai–Tibetan Plateau in a summer. One can note that the differences are significant.

## 5. Conclusions

Based on the data of ‘the Dunhuang Experiment’, the bulk momentum transfer coefficient ( $C_d$ ) and the bulk sensible heat transfer coefficient ( $C_h$ ) over the Gobi were calculated using the eddy correlation, aerodynamic and combinatory methods. It was found that there is some difference between the bulk transfer coefficients calculated with the three different methods. However, the average values are very close to each other. The bulk transfer coefficients calculated with the eddy correlation method appear to be more realistic.

The buildings in the south of the observation station have effects on the results. Due to the building effect, the roughness length is unstable and too large in the nighttime (in the case of south wind), while the bulk transfer coefficients from 7:00–9:00 o’clock are extremely large and their diurnal variations are irregular. The averages of the bulk transfer coefficients become small, and their diurnal variations become regular after the building effect being removed. The averages of  $C_d$  and  $C_h$  calculated with the eddy correlation method are  $2.63 \times 10^{-3}$  and  $2.10 \times 10^{-3}$ , and their neutral values are  $0.92 \times 10^{-3}$  and  $1.81 \times 10^{-3}$ . The correlation between the bulk transfer coefficients and the bulk Richardson number  $R_{ib}$  is analogously linear.

The errors in the friction velocity  $u_*$  and the sensible heat  $H$  calculated with the fitted formulae are tolerable. Their standard deviations are 0.06 m/s and  $37.4 \text{ W m}^{-2}$  respectively. The standard deviations of the friction velocity and the sensible heat flux calculated with the averages of the bulk transfer coefficients are slightly different from those calculated with the fitted formulae.

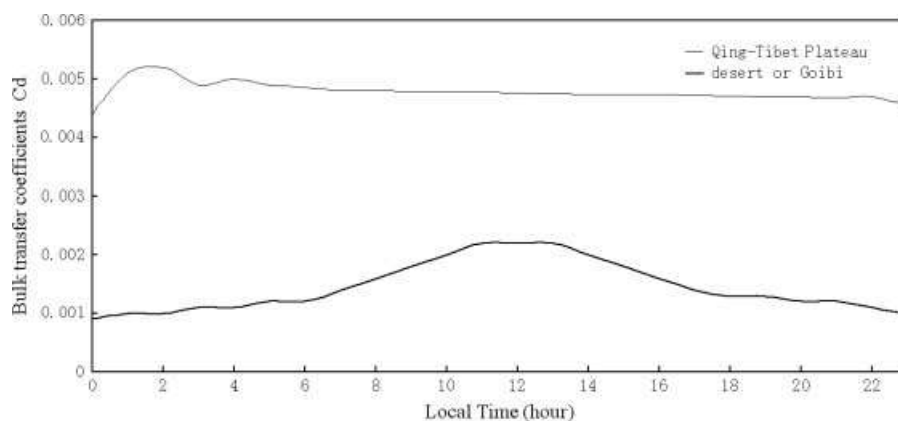


Figure 8. Diurnal variation of momentum bulk transfer coefficients over Gobi in the arid region and over the Qinghai–Tibetan Plateau in a summer.



Because the surface energy balance over the Gobi in arid regions is controlled by the sensible heat flux, the sensible heat transfer coefficients are important with respect to the unique heating effect of arid regions. Due to the special climate and land-surface properties of arid regions, the significant diurnal variation is one of the key characteristics of the bulk transfer coefficients over the Gobi in arid regions.

### Acknowledgements

We thank Professor Wei Guoan, Mr Hou Xuhong, Hu Zeyong, Nie Yanjiang, Gao Hongchong, Zhang Hongmei, Yan Yuping, Wei Zhigang and Hou Ping *et al.* for their assistance in the observation and data procession. We also thank for the comments of the reviewer. This work was supported by the National Natural Science Foundation of China (Grant No. 40830957, 40575006 and 40175004), and the National Key Programme for Basic Sciences – ‘Research on Formation Mechanism and Prediction Theory of Heavy Climatic Disasters in China’ (Grant No. G1998040904-2).

### References

- Businger JA. 1988. A note on the Businger-Dyer profiles. *Boundary-Layer Meteorology* **42**: 145–151.
- Dyer AJ, Hicks BB. 1970. Flux gradient transport of heat and water in an unstable atmosphere. *Quarterly Journal of The Royal Meteorological Society* **93**: 501–508.
- Gao YX. 1990. HEIFE Report (No.1) Preface. *Plateau Meteorology*, 9: Preface.
- Garratt JR. 1977. Review of drag coefficients over Ocean and continent. *Monthly Weather Review* **105**: 915–929.
- Garratt JR. 1992. *The Atmospheric Boundary Layer*. Cambridge University Press: Cambridge.
- Ha S, Dong GR, Wang GY. 1999. Morphology of grid dunes morphology in the southeastern fringe of Tengger Desert – Study of dynamics. *Science in China Series D-Earth Sciences* **42**: 207–216.
- Hicks BB. 1976. Wind profile relationships from the Wangara experiment. *Quarterly Journal of The Royal Meteorological Society* **102**: 535–551.
- Hu YQ, Gao YX, Wang JM. 1994. Some achievements in scientific research during HEIFE. *Plateau Meteorology* **13**: 225–236.
- Hu YQ, Qi YJ. 1991. The combinatory method for determination of the turbulent fluxes and universal functions in the surface layer. *Acta Meteorologica Sinica* **49**: 46–53.
- Hu YQ, Yang XL, Zhang Q. 1992. The characters of energy budget on the Gobi and Desert surface in Hexi Region. *Acta Meteorologica Sinica* **6**: 82–91.
- Li GP, Duan TY, Gong YF. 2000. Bulk transfer coefficient and surface flux on the west of Tibetan plateau. *Chinese Science Bulletin* **45**: 1221.
- Sorbjan Z. 1989. *Structure of the Atmospheric Boundary Layer*. Prentice-Hall, Inc.: Englewood Cliffs, NJ.
- Stull RB. 1988. *An Introduction to Boundary Layer Meteorology*. Kluwer Academic Publishers: The Netherlands.
- Thom AS, Stewart JB, Oliver HR, Gash JHC. 1975. Comparison of aerodynamical and energy budget estimates of fluxes over a pine forest. *Quarterly Journal of The Royal Meteorological Society* **101**: 93–105.
- Wang JM, Liu Xh, Ma YM. 1991. Turbulence structure and transfer characteristics in the surface layer of the HEIFE Gobi area. *Journal of the Meteorological Society of Japan* **69**: 587–593.
- Yao TD. 1999. Climatic change of Tibetan plateau in the last glacial age. *Science in China Series D-Earth Sciences* **42**: 358–570.
- Ye DZ, Gao YX. 1979. *Meteorology of Qinghai-Xizang Plateau*. Science Press: Beijing.
- Zhang Q, Hu YQ. 1992. The instrumental accuracy and observational error about micrometeorological mast of Chinese side in ‘HEIFE’. *Plateau Meteorology* **11**: 460–469.
- Zhang Q, Hu YQ, Wang XH. 1993. Characteristics of micrometeorology over the farmland in oasis in Heihe Region. *Plateau Meteorology* **11**: 361–370.
- Zhang Q, Hu YQ, Yang YF. 1996. The variability process of atmosphere over heterogeneous underlying surface in Hexi region. *Plateau Meteorology* **15**: 282–292.
- Zhang Q, Zhao M. 1999. Field experiment and numerical simulation of inverse humidity of atmosphere over desert near oasis. *Acta Meteorologica Sinica* **57**: 729–740.
- Zhao M, Miao MQ, Wang YC. 1992. *Boundary-Layer Meteorology*. Chinese Meteorology Press: Beijing.
- Zhao P, Chen LX. 2000. The climate characteristics of surface turbulent exchange and surface heat source over the Qinghai-Tibet Plateau. *Acta Meteorologica Sinica* **14**: 13–29.
- Zuo HC, Hu YQ. 1992. The bulk transfer coefficient over Desert and the Gobi in the Heihe region. *Plateau Meteorology* **11**: 371–380.